Numerical simulation of the stamping process for mild steel and GF-PA6 Glass Mat Thermoplastic hybrid assemblies

Oluwajuwon Folorunsho[1,2,a] , Pascal Hubert[1,2,b] and David Trudel-Boucher[3,c]

[1]*Department of Mechanical Engineering, McGill University, QC, Canada*

[2]*Research Center for High Performance and Composite Systems (CREPEC), QC, Canada*

[3]*National Research Council (NRC), Boucherville, QC, Canada*

[a]*oluwajuwon.folorunsho@mail.mcgill.ca,* [b]*pascal.hubert@mcgill.ca,* [c]*david.trudel-boucher@nrc-cnrc.gc.ca*

Keywords: *Mild steel, Glass Mat Thermoplastic (GMT), Hybrid stamping, Coupled Eulerian–Lagrangian (CEL), Finite element simulation.*

1. Abstract

Hybrid stamping of AISI 1008 mild steel and GF-PA6 GMT enables the production of lightweight components in a single stroke. However, predictive simulations remain challenging because metal plasticity and composite squeeze flow occur simultaneously. This study investigates the potential of a coupled Eulerian–Lagrangian (CEL) finite element framework to reproduce the behaviour of mild steel-GMT hybrid assemblies during forming. Material properties were obtained from tensile testing of mild steel, and rheological characterization of GMT samples was performed using a rheometer over a predefined temperature range. Moreover, complementary experimental characterization of GMT was conducted through squeeze-flow compression tests on an MTS 250 kN compression machine under isothermal conditions, and numerical models were developed to model the behaviour of the hybrid metal-thermoplastic assembly. Concurrently, experimental stamping trials at an industrial scale produced critical data to validate the hybrid model. A coupled-hybrid simulation was developed for the same tool geometry used in the experimental stamping trials. Numerical validation showed a very good agreement with data from hybrid stamping trials. Overall, the CEL approach provides a robust predictive framework for investigating the forming behaviour of hybrid metal-thermoplastic assemblies.

2. Introduction

Lightweighting of vehicles, particularly the use of aluminum and magnesium alloys, ultra-high-strength steel, and advanced composite materials, has recently gained significant attention as a measure to reduce greenhouse gas (GHG) emissions from combustion engines and to extend the range of electric vehicles (EVs). In 2018, the transport sector accounted for 25% of Canada's total carbon dioxide emissions, with passenger vehicles and light-duty trucks contributing nearly 50% [1]. Current research has shown that metal-composite hybrids are highly effective for lightweighting, a key approach to significantly reducing GHG emissions. For instance, Jayakumar et al. developed aluminum-Glass Mat Thermoplastic (GMT) crash structures with an approximate 15% weight reduction and high energy absorption capacity [2]. Similarly, Jayasankar et al. fabricated a hybrid brake pedal by in-mould assembly, consisting of GMT cores with steel skins, and achieved a 35% weight reduction [3]. Also, Zhang et al. proposed a combined heat-solid-forming methodology for fibre-reinforced metal laminates, which improves mechanical performance and combines forming and curing into a single process step [4].

Stamp forming, a crucial manufacturing strategy, combines forming and bonding into a single synchronous operation and is among the most promising methods for achieving metal-composite synergy [5]. In this method, not only is production time minimized, but complex structural components for automotive applications can also be manufactured efficiently [5-6]. Building on these developments, the present study focuses on developing a predictive numerical framework for stamping mild steel and GMT composite assemblies. The main objectives of this work are to: (i) experimentally characterize the mechanical and rheological behaviour of the constituent materials under forming-relevant conditions, including tensile testing of steel and squeeze-flow compression tests of GMT; (ii) develop a coupled Eulerian–Lagrangian (CEL) finite element model capable of capturing both the plastic deformation of steel and the flow behaviour of the thermoplastic composite; and (iii) validate the numerical predictions against experimental benchmarks. Through these, the study aims to provide a robust predictive framework that enhances understanding of hybrid forming processes and supports the design and optimization of lightweight metal–thermoplastic components for automotive applications.

3. Materials and Characterization

3.1. Materials

The hybrid laminate consists of a 1.0 mm-thick AISI 1008 mild steel bonded to E-type GF-PA6 GMT, with a nominal thickness of 2.5 mm and a glass-fibre weight fraction of 50%. The GMT blanks supplied by Johns Manville were compression moulded from discontinuous glass-fibre mats, forming quasi-isotropic sheets with random in-plane fibre orientation and an average fibre length of about 25 mm. Fig. 1 illustrates the individual metallic and composite components.

(a) 50% filled GF/PA6 sheet.

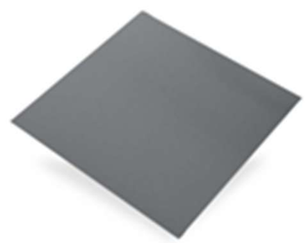

(b) Mild steel sheet

Figure 1. Components of the hybrid laminate.

3.2. Characterization

(a) Tensile characterization of Mild Steel

Ten dog-bone AISI 1008 steel specimens were tested in tension following ASTM E8/E8M to determine their mechanical behaviour. The specimens (12.52 mm × 0.89 mm) were instrumented with a calibrated extensometer, and cross-sectional areas were measured directly. The tests showed high repeatability, with an average peak load of 3534.60 N (±40.54 N). The steel exhibited an average yield stress of 185.42 MPa and an ultimate tensile strength of 318.26 MPa, values consistent with published ranges for mild steel. A high level of ductility was also observed in the material, with an average elongation at fracture of 42.20% (±1.36 %). The excellent formability of AISI 1008 steel yields a favourable stress–strain response, making it ideal for hybrid metal–thermoplastic uses. These experimentally derived stress-strain and modulus characteristics were subsequently implemented as input parameters for finite element simulations to define the steel response in the hybrid GMT-steel assembly.

(b) GMT Composite Characterization

(i) Rheological Characterization of GMT Composites

Dynamic oscillatory shear tests were conducted on a TA Instruments Anton-Parr MCR 302 rheometer using a 25-mm parallel-plate configuration. A frequency sweep (0.1–10 Hz) was performed at 210°C-260°C under isothermal conditions, following a similar approach by Dorr et al. [7]. The storage (G') and loss (G'') moduli were measured and fitted to determine the viscoelastic behaviour of GMT composites. The corresponding complex viscosity as a function of shear rate is presented in Fig. 2. To enable comparison with steady-shear behaviour, the Cox–Merz rule was employed to convert oscillatory data into equivalent shear-rate-dependent viscosities. The results reveal strong shear-thinning behaviour, which is typical of thermoplastic composites in the molten state and becomes especially important under the high local deformation rates.

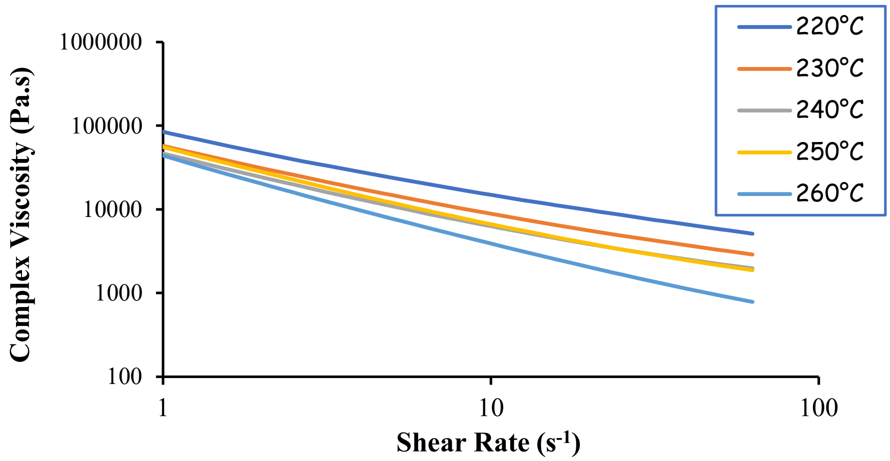

Figure 2. A graph of complex viscosity against shear rate at 210°C – 260°C of GF/PA6.

(ii) Squeeze Flow Compression Testing

To estimate the bulk response of the GMT composite under forming conditions, squeeze-flow experiments were conducted in displacement-control mode at 240°C using an MTS 250 kN compression machine [8]. Fig. 3 illustrates a schematic of the squeeze-flow compression process. The initial sample was dimensioned 101.6 mm × 25.4 mm, and its thickness was measured at 4 mm before compression. A *Zyvax Compositeshield* release agent was applied to the platens of the 101.6 mm square mould to minimize sticking, left to dry for 15 minutes, and then the mould was heated to 240°C. The sample was inserted into the mould, the platen brought to a 4mm platen gap, and the sample left for 3 minutes to reach the required testing temperature. Compression was initiated at a crosshead speed of 0.1 mm/s until a thickness of 1.27mm was achieved. The relaxation data and force-gap response of the composite were collected, and the final thickness was also measured manually using a vernier calliper. The difference between the measured final thickness and the final thickness collected from the DAQ software was less than 5%.

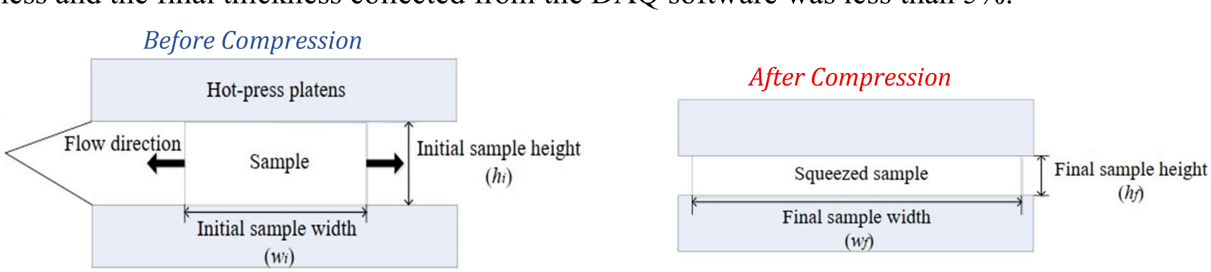

Figure 3. Schematic of a Squeeze Flow Test before and after compression. [8]

4. Hybrid Numerical Model

4.1. Modelling Strategy

The hybrid forming process was simulated using a two-stage numerical framework within Abaqus/Explicit. In the first stage, the deformation of the steel and composite sheets was modelled using the setup in Fig 4, and a purely Lagrangian formulation to capture the initial structural response, including bending and stretching. The Lagrangian elastoplastic formulation enables accurate prediction of bending, thinning, and corner deformations under forming conditions [9]. A viscosity-based strategy, adapted from Dorr et al. and calibrated using the squeeze flow response from the experiment in section 3.0 above, was used to describe the thermoplastic composite, thereby capturing shear-thinning, compressibility, and complex deformations [7]. Finally, in the second stage, the deformed hybrid geometry, together with the associated solution-dependent variables, was mapped into a CEL framework, as described in Fig. 5. This approach enabled the simultaneous simulation of metal deformation and thermoplastic composite flow within a unified computational domain.

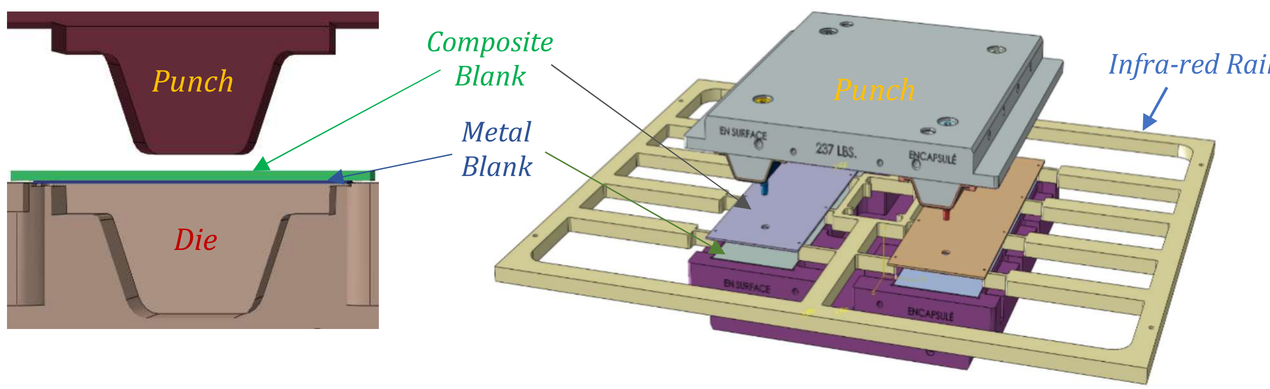

Figure 4. Hybrid model set-up (without the Eulerian domain) illustrating the punch, blank, and die set-up that incorporates the steel and GMT blank.

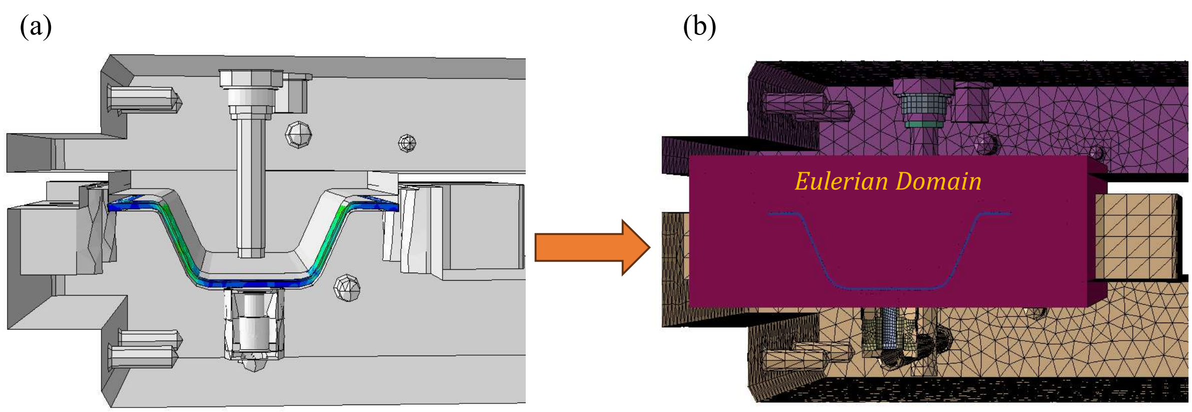

Figure 5. Geometry transfer from the Stage 1 Lagrangian forming simulation to the Stage 2 coupled Eulerian–Lagrangian (CEL) model for hybrid stamp forming.

Within the CEL formulation, the steel sheet was treated as a Lagrangian body, while the thermoplastic composite was initialized in a Eulerian domain encapsulating the combined composite and metal blanks. This hybrid approach eliminates mesh distortion typically associated with large deformations in purely Lagrangian simulations and provides a physically consistent representation of metal–polymer interaction during forming.

4.2. Governing Equations and Constitutive Models

Both mild steel and GMT composite materials are governed by the fundamental balance of momentum for a deforming continuum in the hybrid, as expressed in Equation 1:

$$\rho \frac{D\mathbf{v}}{Dt} = \nabla \cdot \boldsymbol{\sigma} + \rho \mathbf{b} \tag{1}$$

where ρ is the material density, $\mathbf{v}$ is the velocity field, $\boldsymbol{\sigma}$ is the Cauchy stress tensor, and $\mathbf{b}$ represents body forces.

The stress tensor is decomposed into hydrostatic pressure and deviatoric stress components as in Equation 2:

$$\boldsymbol{\sigma} = -p\mathbf{I} + \boldsymbol{\tau} \tag{2}$$

where p is the pressure, $\mathbf{I}$ is the identity tensor, and $\boldsymbol{\tau}$ represents the deviatoric stress tensor. Within the hybrid model, the constitutive behaviour of the two materials is described using different stress relations. The steel sheet follows an elastic–plastic constitutive formulation based on the additive decomposition of strain as summarized in Equation 3:

$$\boldsymbol{\varepsilon} = \boldsymbol{\varepsilon}_e + \boldsymbol{\varepsilon}_p \tag{3}$$

where $\boldsymbol{\varepsilon}_e$ and $\boldsymbol{\varepsilon}_p$ denote the elastic and plastic strain components, respectively. Plastic deformation occurs when the stress state satisfies the chosen yield criterion and evolves according to the associated hardening law.

In contrast, the molten thermoplastic composite behaves as a viscous material whose deviatoric stress is governed by the generalized Newtonian fluid relation in Equation 4:

$$\boldsymbol{\tau} = 2\eta(\dot{\gamma})\mathbf{D} \tag{4}$$

where $\eta(\dot{\gamma})$ is the shear-rate-dependent viscosity defined through the Carreau–Yasuda rheological model and $\mathbf{D}$ is the rate-of-deformation tensor.

Furthermore, Equation 5 describes the interaction between the metal sheet and the flowing composite via contact constraints that ensure traction continuity at the interface.

$$\boldsymbol{\sigma}_m \cdot \mathbf{n} = \boldsymbol{\sigma}_c \cdot \mathbf{n} \tag{5}$$

where $\mathbf{n}$ is the interface normal, and the subscripts $\boldsymbol{m}$ and $\boldsymbol{c}$ denote the metal and composite domains, respectively. This condition ensures that stresses transmitted across the metal–composite interface remain in equilibrium during deformation.

4.3. Composite Material Modelling

Three fundamental variables were specified to completely define the behaviour of the GMT composite: viscosity, the equation of state (EOS), and density. All these parameters, when considered with temperature, govern the thermo-mechanical behaviour of the GMT material during the forming process and are therefore essential for process simulation. The viscosity model plays a central role in describing the composite's flow behaviour under deformation. Notably, the viscosity data obtained for isothermal rheological testing at 240°C were fitted using the Carreau–Yasuda model to estimate viscosity as a function of shear rate, **$\eta(\gamma)$,** and is expressed in Equation 6 as:

$$\eta(\gamma) = \eta_\infty + (\eta_\circ - \eta_\infty)\,[1 + (\lambda\gamma)^a\,]^{\frac{(n-1)}{a}} \tag{6}$$

where **η_0** (MPa·s) is the zero-shear viscosity, **$\eta\infty$** (MPa·s) is the infinite-shear viscosity, **λ (s)** is the time constant controlling the shear-rate transition, **n** is the power-law index for the slope of the shear-thinning region, and **a** is the Yasuda parameter controlling the width of the transition region.

The graph of the model fit is shown in Fig. 6, and the fitted parameters yielded a zero-shear viscosity of **η_0** = 0.282 MPa·s, corresponding to the highly viscous Newtonian plateau observed at low shear rates, and an infinite-shear viscosity of **$\eta\infty$** = 0.001135 MPa·s**,** representing the asymptotic viscosity at high shear rates. The transition between these regimes was governed by a characteristic time constant of **λ** = 6.8348 s. Pronounced shear-thinning behaviour was captured by a power-law index of **n** = 0.0524. At the same time, the Yasuda parameter, set to **a** = 10.0, controlled the width of the transition region between the Newtonian and shear-thinning domains. This model was later implemented in Abaqus using tabulated viscosity functions, thereby enabling an accurate representation of the experimentally observed shear-rate-dependent flow behaviour.

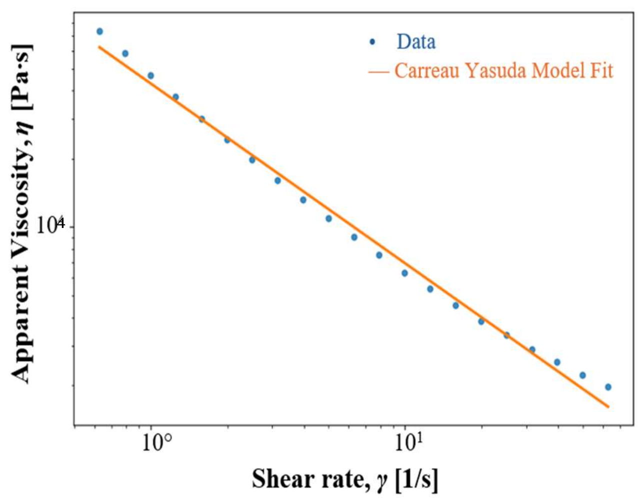

Figure 6. Apparent viscosity as a function of shear rate for the sheet at 240 °C, showing the experimental data and the Carreau–Yasuda model fit.

An equation of state (EOS) was also incorporated to characterize the compressibility or pressure–volume–temperature (PVT) behaviour of the thermoplastic composite matrix, which becomes significant when the molten material is forced into a confined cavity during stamp forming, resulting in substantial pressure buildup. In this study, the EOS was derived from experimental PVT data for PA6 reported by Utracki [10] at 240°C and employed to develop an isothermal numerical model. Since the PA6 matrix governs the compressibility of the GMT composite in its molten state, the use of Utracki's PVT data proved particularly valuable. Generally, the PVT response of PA6 exhibits a nonlinear decrease in specific volume with increasing pressure and a clear temperature dependence, with higher temperatures yielding greater specific volumes at a given pressure.

4.4. Contact and Interaction

General contact interactions were defined between the punch, die, steel sheet, and GMT blank to ensure continuous load transfer throughout the forming process. As the punch advances, the steel sheet bends and stretches, while the molten composite flows within the die cavity under pressure. At the metal–composite interface, a frictionless contact formulation was adopted as an initial simplification, allowing relative sliding without resistance. This assumption enables stable numerical convergence while capturing the primary load transfer mechanism between the two materials. Interactions between the tooling and the workpieces were also defined within the general contact framework. Traction continuity was enforced at the interface to ensure stress equilibrium between the deforming metal and the flowing composite. This guarantees a physically consistent coupling between the Lagrangian steel and Eulerian GMT composites within the CEL formulation.

4.5. Assumptions and Simplifications

Realistic boundary conditions were imposed by fixing the die in all degrees of freedom while restricting the punch to vertical motion only. To ensure computational efficiency while retaining the dominant physical mechanisms governing the hybrid forming process, several simplifying assumptions were introduced. All simulations were conducted under isothermal conditions at 240°C. Consequently, heat transfer between the tooling and the workpieces, latent heat effects associated with melting or crystallization, and temperature gradients through the material thickness were neglected. The steel sheet was assumed to remain at a uniform temperature, and temperature-dependent elastoplastic properties were not considered. This is justified because the steel response is predominantly mechanical, and its strength at the forming temperature remains relatively high compared to that of the softened composite. The thermoplastic composite was modelled using a homogenized continuum approach in which the reinforcing glass fibres were not explicitly resolved. Microscale mechanisms such as fibre bending, breakage, and reorientation were therefore not directly simulated. Instead, their overall influence was incorporated implicitly through the calibrated viscosity model and the equation of state. This approximation is appropriate for macroscopic simulations where bulk material flow dominates. The tooling was modelled as perfectly rigid because it has significantly higher stiffness than the deforming materials. Finally, quasi-static conditions were enforced using explicit time integration. Inertia effects were minimized, and numerical mass scaling was avoided to preserve the physically meaningful rate-dependent behaviour of the GMT composite.

4.6. Geometry and Meshing

A Lagrangian elastoplastic formulation with the von Mises yield criterion and isotropic hardening was employed to model the 1-mm-thick steel sheet. The constitutive parameters were calibrated from uniaxial tensile tests described in Section 3.2a and implemented to accurately reproduce the experimentally observed stress–strain response under forming conditions. The steel blank was defined with the same dimensions as the experimental specimen (456.692 mm × 136.432 mm × 1 mm), ensuring direct geometric correspondence between numerical and physical configurations. The sheet was discretized using 8-node linear hexahedral elements with incompatible modes (C3D8I), which provide enhanced accuracy in bending-dominated problems by improving strain interpolation and mitigating shear locking effects. A structured mesh was applied, and a single element was assigned through the thickness to ensure consistent plastic strain localization and maintain numerical stability under large-deformation bending. The thermoplastic composite was modelled within a Coupled Eulerian–Lagrangian (CEL) framework using EC3D8R reduced-integration Eulerian brick elements. The composite charge, initially dimensioned as 456.184 mm × 150.664 mm × 2.9 mm, was first deformed together with the steel sheet in the Lagrangian stage and subsequently mapped into a rectangular Eulerian domain in the second stage of the simulation.

The Eulerian domain (475 mm × 177.8 mm × 64 mm) was intentionally defined with enlarged lateral and vertical extents relative to the initial blank geometry to accommodate unrestricted material flow, free-surface evolution, and cavity filling without artificial boundary confinement. Within the Eulerian formulation, the initial composite region was defined using a Eulerian Volume Fraction (EVF) equal to unity, while surrounding void regions were assigned a value of zero, enabling accurate representation of free surfaces and preventing numerical diffusion during large-deformation flow. The global element size of the Eulerian mesh was set to 0.7 mm based on uniform seeding. To improve geometric fidelity in regions of high curvature and intense material flow, curvature control was applied with a maximum deviation factor of 0.1, corresponding to approximately eight elements per circular arc. Local mesh refinement was introduced by setting a minimum element size of 10% of the global seed size (≈0.07 mm), thereby enhancing resolution in tool–material interaction zones and in regions exhibiting steep velocity and pressure gradients.

5. Model Validation and Results

5.1. Experimental Forming Trials

To validate the numerical model, experimental forming trials were carried out at the National Research Council (NRC) composite forming laboratory using hybrid steel–composite assemblies. The facility is equipped with a 1250-ton hydraulic press, an infrared heating oven, and an automated transfer system manufactured by Pinette Emidecau Industries (PEI). For composite forming, the GMT blank was placed on the transfer shuttle, heated in the infrared oven to 250 °C, and then rapidly transferred to the forming tool. Stamping was performed under a load of 125 tons with a dwell time of 25 s. Due to transfer-induced heat loss, the composite temperature stabilized at approximately 240 °C upon contact with the tool. The die temperature was actively controlled at 80 °C throughout all trials to ensure repeatable thermal conditions. For hybrid forming, the GMT sheet was positioned over a pre-placed steel blank within the die cavity. The metallic insert was accurately located using guiding pins integrated into the punch, which engaged pre-cut openings in the steel sheet to ensure positional stability during forming. The assembly was then stamped under identical processing conditions (Fig 7). After forming, the components were inspected to evaluate cavity filling, void formation, and global deformation behaviour. These observations provide the experimental basis for validating the FE model, particularly in predicting composite squeeze flow, pressure evolution, and metal–composite interaction during hybrid stamping.

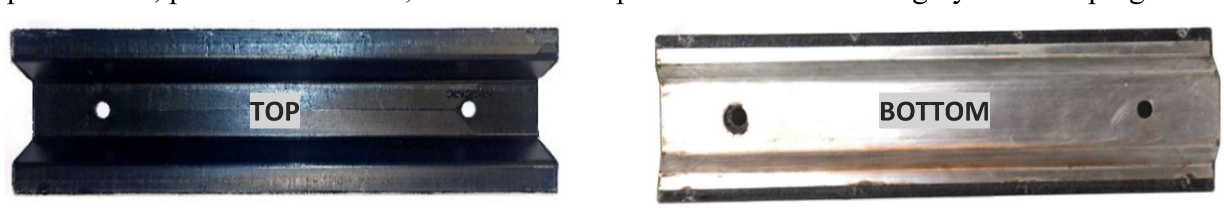

Figure 7. Experimental forming trials of an AISI 1080 steel-GF50/PA6 hybrid part.

5.2. Numerical Results, Comparison and Validation

Following the numerical simulation, the predicted response of the hybrid system was analyzed to evaluate the evolution of metal deformation and thermoplastic composite flow during the forming process. The simulation results, shown in Fig. 8, provide insight into the interaction mechanisms between the steel insert and the molten GMT composite under forming conditions.

Material distribution within the Eulerian domain was quantified using the Eulerian Volume Fraction (EVF), which describes the local occupancy of composite material in each Eulerian element. EVF values below unity indicate partially filled regions resulting from free-surface evolution rather than porosity or material loss. The hybrid model, therefore, captures the essential physics of metal–polymer interaction by combining metal deformation and composite squeeze-flow redistribution within a fully coupled CEL simulation framework.

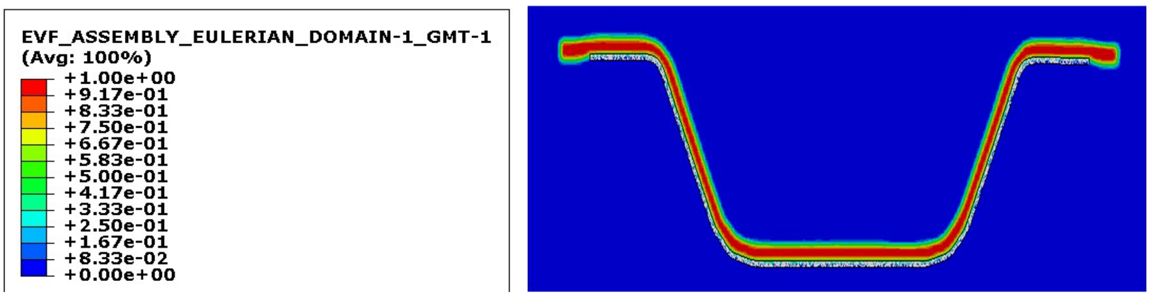

Figure 8. Eulerian Volume Fraction (EVF) contours showing the predicted redistribution of the molten GMT composite around the steel insert during hybrid stamp forming.

Validation of simulation results for the hybrid component was conducted by comparing the predicted cross-sectional profile and thickness distribution with experimental results, as shown in Fig. 9. The simulation reproduced the overall formed geometry with good agreement, accurately capturing the bending of the steel insert and the redistribution of the molten composite around it. Thickness validation at 11 measurement locations also showed strong agreement, with exact prediction at 5 locations, an average deviation of approximately 3%, and a maximum deviation of 9.09% in the inclined sidewall transition regions. These results demonstrate that the model can reliably predict both the global shape and the local thickness evolution of the stamped hybrid.

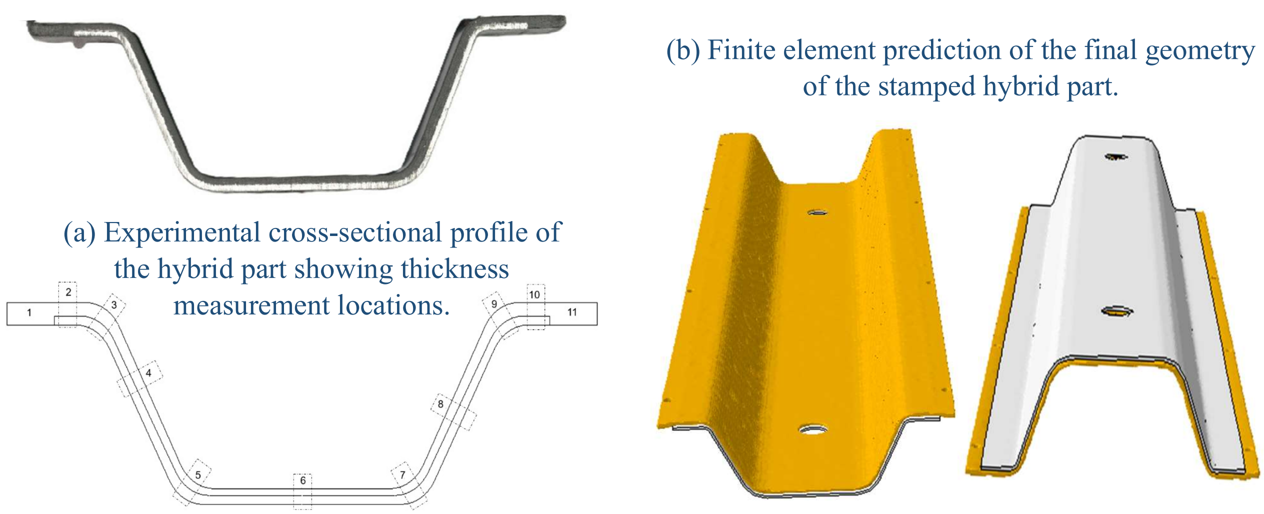

Figure 9. Hybrid model validation: (a) experimental cross-sectional profile with thickness measurement locations; (b) FE-predicted final geometry of the stamped hybrid part.

6. Conclusion

This study demonstrates that hybrid stamping can effectively form metal–thermoplastic structures by simultaneously deforming the steel sheet and the molten composite. The developed CEL model also enabled visualization of the composite flow and pressure buildup during forming, providing useful insights into the deformation behaviour of thermoplastics in the hybrid process. Although the model assumes an isothermal process and neglects interfacial adhesion, the results highlight the strong potential of CEL-based modelling as a predictive tool for understanding and designing hybrid forming processes. Future work will incorporate temperature-dependent viscosity, interfacial thermomechanical effects, and anisotropic composite behaviour, and extend the methodology to larger demonstrator components for automotive applications.

7. References

[1] A. Munzur, Canada's GHG Emissions from Transportation and Electricity Sectors, The School of Public Policy, University of Calgary, 2021. Link: EEPT-August-2021-FINAL.pdf

[2] S. Jayakumar, A. Hajdarevic, S.C. Anand, X.F. Fang, Experimental and FE analyses of the crushing and bending behaviours of GMT and hybrid-formed Al-GMT structures, Thin-Walled Struct. 186 (2023) 110648. DOI: 10.1016/j.tws.2023.110648

[3] D. Chalicheemalapalli Jayasankar, T. Stallmeister, J.J. Lückenkötter, T. Tröster, T. Marten, Process development for hybrid brake pedals using compression molding with integrated in-mold assembly, Polymers 17 (2025) 1644. DOI:10.3390/polym17121644

[4] Q. Zhang, F. Sun, Y. Ma, Z. Sun, The experimental study on the mechanical properties of fibre-reinforced metal laminates using an innovative heat-solid integrated forming technology, Metals 13 (2023) 1199. DOI: 10.3390/met13071199

[5] L. Mosse, P. Compston, W. J. Cantwell, M. Cardew-Hall, S. Kalyanasundaram, Stamp forming of polypropylene based fibre–metal laminates: The effect of process variables on formability, J. Mater. Process. Technol. 172 (2006) 163–168. DOI: 10.1016/j.jmatprotec.2005.09.002

[6] M. Smolnicki, Z. Grządziel, A. Komorek, Ł. Bąk, A review on finite-element simulation of fibre metal laminates, Archives of Computational Methods in Engineering. (2023). DOI: 10.1007/s11831-022-09814-8

[7] D. Dörr, N. Singh-Heer, R.C.R. Gergely, L. Schreyer, F. Henning, A.G. Straatman, A. Hrymak, Rheological characterization and macroscopic modeling and simulation of the molding process of a PA6 Glass Mat Thermoplastic (GMT), Compos. Part A 176 (2024) 107780. DOI: https://doi.org/10.1016/j.compositesa.2023.107780

[8] G. Picher-Martel, A. Lévy, P. Hubert, Compression moulding of carbon/PEEK randomly-oriented strands composites: a 2D finite element model to predict the squeeze flow behaviour, Compos. Part A 81 (2016) 69–77. DOI: 10.1016/j.compositesa.2015.11.006

[9] Y. Hou, D. Myung, J.K. Park, J. Min, H.R. Lee, A. Abd El Aty et al., A review of characterization and modelling approaches for sheet metal forming of lightweight metallic materials, Materials 16 (2023) 836. DOI: 10.3390/ma16020836

[10] L.A. Utracki, Equations of state for polyamide-6 and its nanocomposites. 1. Fundamentals and the matrix, J. Polym. Sci. Part B: Polym. Phys. 47 (2009) 299–313. DOI: 10.1002/polb.21640